Naval Research Laboratory

Washington, DC 20375-5320

NRL/FR/6840--97-9845

CHRISTINE: A Multifrequency Parametric Simulation Code for Traveling Wave Tube Amplifiers

THOMAS M. ANTONSEN, JR.

Science Applications International Corporation
McLean, VA

BARUCH LEVUSH

Vacuum Electronics Branch
Electronics Science and Technology Division

May 5, 1997

REPORT DOCUMENTATION PAGE

Form Approved
OMB No. 0704-0188

1. AGENCY USE ONLY (*Leave Blank*)	2. REPORT DATE	3. REPORT TYPE AND DATES COVERED
	May 5, 1997	FINAL; January 1996 to April 1997

4. TITLE AND SUBTITLE

CHRISTINE: A Multifrequency Parametric Simulation Code for Traveling Wave Tube Amplifiers

5. FUNDING NUMBERS

WU - 6410
7234
PE - 34-1-08

6. AUTHOR(S)

Thomas M. Antonsen, Jr.* and Baruch Levush

7. PERFORMING ORGANIZATION NAME(S) AND ADDRESS(ES)

Naval Research Laboratory
Washington, DC 20375-5320

8. PERFORMING ORGANIZATION REPORT NUMBER

NRL/FR/6840--97-9845

9. SPONSORING/MONITORING AGENCY NAME(S) AND ADDRESS(ES)

Office of Naval Research
800 North Quincy Street
Arlington, VA 22217-5660

10. SPONSORING/MONITORING AGENCY REPORT NUMBER

11. SUPPLEMENTARY NOTES

* Science Applications International Corporation, McLean, VA 22102
Permanent address: Departments of Electrical Engineering and Physics, University of Maryland, College Park, MD 20742

12a. DISTRIBUTION/AVAILABILITY STATEMENT

Approved for public release; distribution unlimited.

12b. DISTRIBUTION CODE

13. ABSTRACT (*Maximum 200 words*)

A model and computer code are presented that simulate the operation of traveling wave tube amplifiers (TWTs). The model is based on the well-known parametric theory in which the relevant properties of the interaction circuit are the phase velocity and coupling impedance of the waves supported by the slow wave structure. The model includes a multifrequency description of both the fields of the structure and the space charge fields. This allows for the study of harmonic and intermodulation distortion. The beam is treated as an ensemble of disks with an effective axial velocity spread. Several options are available for specifying the parameters of the interaction circuit: using a sheath helix description, importing data from another model, or using data from experimental measurement. The advantages of the code are that it can relatively quickly simulate situations in which the amplifier is driven by multiple input frequencies, it is readily portable to different platforms, and it facilitates tube design by enabling users to vary parameters relatively easily.

14. SUBJECT TERMS			15. NUMBER OF PAGES
Traveling wave tubes	Large signal code	Intermodulation	39
			16. PRICE CODE

17. SECURITY CLASSIFICATION OF REPORT	18. SECURITY CLASSIFICATION OF THIS PAGE	19. SECURITY CLASSIFICATION OF ABSTRACT	20. LIMITATION OF ABSTRACT
UNCLASSIFIED	UNCLASSIFIED	UNCLASSIFIED	UL

NSN 7540-01-280-5500

Standard Form 298 (Rev. 2-89)
Prescribed by ANSI Std 239-18
298-102

CONTENTS

CHRISTINE: A MULTIFREQUENCY PARAMETRIC SIMULATION CODE FOR TRAVELING WAVE TUBE AMPLIFIERS

1. INTRODUCTION

In many applications of traveling wave tube amplifiers (TWTs) in the defense arena, including electronic warfare (EW), radar, and communications, TWTs are required to amplify multiple frequencies simultaneously. In these applications, nonlinearities in the amplification process cause intermodulation and amplitude and phase cross-modulation. When the number of carriers is large, this phenomenon becomes even more complex. Existing tubes avoid these parasitic effects by combining such techniques as feed-forward compensation or operation in the linear regime with depressed energy collection of the electron beam. Associated with these techniques is the cost of increasing the complexity of the tube or the weight of the power supply. Some EW applications require intermodulation products at levels no greater than -30 to -40 dBc and phase stability less than 3°/dB. Communication applications can require intermodulation levels as low as -70 dBc. Moreover, the requirement to further increase the efficiency, frequency, and power level of TWTs makes attaining these levels of intermodulation and cross-modulation even more difficult. Thus, interest has been refocused on designing TWTs that minimize intermodulation and cross-modulation distortion.

This report describes the workings of a parametric computer code, CHRISTINE, that models the operation of TWTs in the presence of multiple frequency signals. The report provides examples of how CHRISTINE can be used and serves as a user's guide to the model. The basic model is a variation of that which has been in use in the field for some time [1-4]. We have attempted to keep the notation as similar as possible to that of the basic equations of classical physics. The parametric description of the complex interaction between the particles and fields in a TWT is not all inclusive as is, say, that of a particle in cell code. However, CHRISTINE can quickly calculate the output spectrum of a device with many frequencies present. As such, it is useful in designing devices where many simulations are required to cover a large parameter space.

Section 2 of this report describes the physical model, which forms the basis for the code. The discussion is general enough to provide a user of the code a good understanding of which processes are being simulated. Section 3 describes some of the numerical methods used in solving the basic equations and discusses the organization of the code and the functions of the various subroutines. Section 4 provides a set of examples that illustrate the workings of the code, the input parameter namelists and files, and the output files.

2. PHYSICAL MODEL

2.1 The Electromagnetic Fields of the Structure and Their Frequencies

We begin the description of the physical model employed in CHRISTINE with the representation of the assumed fields of the cold structure. Ultimately, in the type of model presented here, only two frequency dependent quantities—the phase velocity and the coupling impedance—are needed to specify the parameters of the cold structure fields. We begin, however, at a more basic level to underscore the nature of the approximations being made.

Manuscript approved Oct. 21, 1996.

The fields of the structure are represented in the form of the product of a slowly varying, complex amplitude δA_n, periodic eigenfunctions $\boldsymbol{e}_n(\boldsymbol{x})$ and $\boldsymbol{b}_n(\boldsymbol{x})$, and an exponential phase factor,

$$\boldsymbol{E}_{rf}(x,t) = \sum_n i \frac{\omega_n}{c} \delta A_n(z)\, \boldsymbol{e}_n(\boldsymbol{x})\, exp\,[i(\int_0^z k_{zn}(z')\,dz' - \omega_n t)] + c.c. \tag{1a}$$

and

$$\boldsymbol{B}_{rf}(x,t) = \sum_n i \frac{\omega_n}{c} \delta A_n(z)\, \boldsymbol{b}_n(\boldsymbol{x})\, exp\,[i(\int_0^z k_{zn}(z')\,dz' - \omega_n t)] + c.c.\ . \tag{1b}$$

Here it is assumed that $\boldsymbol{e}_n(\boldsymbol{x})$ and $\boldsymbol{b}_n(\boldsymbol{x})$ are the solutions of Maxwell's equations for the empty structure corresponding to angular frequency ω_n and real axial wave number k_{zn}. In this regard, $\boldsymbol{e}_n(\boldsymbol{x})$ and $\boldsymbol{b}_n(\boldsymbol{x})$ will be periodic in axial distance with a period equal to that of the structure. To allow for the slow axial variation of the structure's parameters, the wave number k_{zn} corresponding to frequency ω_n as well as the eigensolutions $\boldsymbol{e}_n(\boldsymbol{x})$ and $\boldsymbol{b}_n(\boldsymbol{x})$ will vary with axial distance. It is assumed that such variations are slow and that it is permissible to think of the functions $\boldsymbol{e}_n(\boldsymbol{x})$ and $\boldsymbol{b}_n(\boldsymbol{x})$ as being locally periodic. As Maxwell's equations for the cold structure are linear, we can take the eigensolutions $\boldsymbol{e}_n(\boldsymbol{x})$ and $\boldsymbol{b}_n(\boldsymbol{x})$ to be dimensionless. In this case, the slowly varying amplitude δA_n has the dimensions of a vector potential.

The sum over the subscript n in Eqs. (1a) and (1b) represents a sum over frequencies ω_n. Note that all the time dependence of the fields is contained in the exponential factors; that is, the amplitudes δA_n depend only on axial distance. This representation of the field corresponds to the case in which the device is excited by a signal consisting of a discrete set of frequencies belonging to the set ω_n. In CHRISTINE, all frequencies are assumed to be integer multiples of some minimum frequency $\Delta\omega$. In this case, the nonlinear beating of any two signals in the device will produce a signal at a frequency that is a member of the set ω_n. This beating could be in the form of self-beating, which would generate harmonic frequencies, or it could be in the form of beating of two signals of different frequency, which would generate intermodulation distortion. The restriction that members of the set ω_n are integer multiples of some minimum frequency $\Delta\omega$ can be stated in another way. The input signal and all other quantities of interest are assumed to be periodic in time with period $T = 2\pi/\Delta\omega$. Section 2.2 discusses the implications of this for the injection of particles in the simulation.

The time-averaged electromagnetic power flux along the structure implied by Eqs. (1a) and (1b) can be evaluated using Poynting's theorem,

$$P = \frac{c}{2\pi} \sum_n \left| \frac{\omega_n}{c} \delta A_n(z) \right|^2 A_{eff,n}\,, \tag{2}$$

where $A_{eff,n}$ is the effective cross-sectional area defined by the relation

$$A_{eff,n} = \frac{1}{2} \int d^2x_\perp\ \hat{z} \cdot (\boldsymbol{e}_n^* \times \boldsymbol{b}_n + \boldsymbol{e}_n \times \boldsymbol{b}_n^*) \tag{3}$$

and $\hat{z}$ is a unit vector in the axial direction. For a structure with slowly varying parameters, the contribution to the power flux from each frequency (i.e., each term in the sum in Eq. (2)) will be independent of axial distance in the absence of a beam or attenuation. Basically, this assumes that the parameters are tapered gently enough so that the amount of power reflected from a forward

propagating wave is negligibly small. With tapering, the quantity $A_{eff,n}$ will vary with axial distance as the parameters of the structure vary. Consequently, according to Eq. (2), in a structure with slowly varying parameters, the amplitude δA_n will vary with axial distance even if the power flux is constant. To account for this, we introduce a normalized field amplitude

$$a_n(z) = \frac{\omega_n}{c} \frac{q\, \delta A_n(z)}{mc^2} A_{eff,n}^{1/2}, \tag{4}$$

where q and m are the charge and mass of an electron, respectively. The code determines the dimensionless quantity a_n. This choice of normalization gives the following expression for the power flux:

$$P = P_{flux,2} \sum_n |a_n(z)|^2, \tag{5}$$

where

$$P_{flux,2} = \frac{c}{2\pi} \left(\frac{mc^2}{q}\right)^2 = 1.3862 \times 10^9 \ watts \tag{6}$$

is a constant. A consequence of normalization is that under the stated assumptions, specifically the negligibly small reflection of forward propagating power, a_n varies because of attenuation and coupling to the beam, not because of the structure's slowly changing parameters.

The complex amplitude is derived by following these standard steps. Expressions (1a) and (1b) are inserted in Maxwell's equations along with the beam current. Ampere's law is dotted with $\boldsymbol{e}_n^*(\boldsymbol{x})$ and Faraday's law is dotted with $\boldsymbol{b}_n^*(\boldsymbol{x})$. The two products are combined in the same way as one forms Poynting's theorem, and the resulting expression is averaged over the spatial period of the structure and the temporal period T of the fields. Weak attenuation is introduced by the boundary condition that the tangential electric field of the radiation does not quite vanish on the structure walls. Thus, the resulting equation for the amplitude of the n^{th} spectral component is

$$\left(\frac{d}{dz} + \alpha_n(z)\right) a_n = \frac{2\pi i}{I_A A_{eff,n}^{1/2}} \left\langle \int d^2x_\perp \, \boldsymbol{j} \cdot \boldsymbol{e}_n^*(\boldsymbol{x}) \, exp\,[-i(\int_0^z k_{zn}(z')\, dz' - \omega_n t)] \right\rangle, \tag{7}$$

where $\alpha_n(z)$ is the attenuation in Nepers/cm and is frequency dependent, $I_A = mc^3/q$, $\boldsymbol{j}$ is the beam current density, and the angular brackets denote averages over the temporal period of the radiation and the spatial period of the structure. The right-hand side of Eq. (7) is further refined in Section 2.2 after a discussion of the equations of motion.

2.2 Equations of Motion

In CHRISTINE, beam electrons are treated as annular discs of charge of outer radius r_{bo} and inner radius r_{bi} which are constrained to move in only the axial direction. One expects this approximation to be appropriate when the electrons are confined by either a strong axial magnetic field or a system of periodic focusing magnets. The motion of the electrons will be one dimensional if the frequency of the amplified signal is much smaller than the frequency of particle oscillations in the relevant confining field (the gyrofrequency or the betatron frequency). The disc approximation will be appropriate if the axial electric field of the signal does not vary appreciably over the radial extent of the electron beam.

The rate of change of electron energy is expressed in terms of the rate of change of the relativistic factor $\gamma = 1/\sqrt{1 - v^2/c^2}$,

$$\frac{d\gamma}{dz} = \frac{q}{mc^2} \left\langle \hat{z} \cdot \left(\boldsymbol{E}_{rf} + \boldsymbol{E}_{sc} + \boldsymbol{E}_{dc} \right) \right\rangle_{beam} . \tag{8}$$

Here, $\boldsymbol{E}_{rf}$ is the electric field of the structure field given by Eq. (1a), $\boldsymbol{E}_{sc}$ is the AC space charge field discussed in Section 2.3, and $\boldsymbol{E}_{dc}$ is a steady-state axial electric field, if present, that changes the energy of beam electrons as they travel through the structure. A steady-state axial field will be present if the DC space charge depression varies with axial distance (e.g., if the parameters of the structure are tapered). Equation (8) describes the Lagrangian rate of energy change of a particle as it travels down the interaction region. The independent coordinate is the axial location of an electron. To determine the arrival time $t(z)$ of an electron at a particular axial location, we solve

$$\frac{dt}{dz} = \frac{1}{v_z(\gamma)} , \tag{9}$$

where the axial velocity of an electron is given in terms of the relativistic factor γ and the pitch factor Θ is

$$v_z(\gamma) = c \left(1 - \frac{1 + (\gamma_0^2 - 1)\,\Theta^2}{\gamma^2} \right)^{1/2} . \tag{10}$$

The pitch factor Θ is the ratio of the transverse component to the total momentum on injection and γ_0 is the electron's relativistic factor on injection. The model assumes that $\Theta << 1$, i.e., small enough so that the motion is one dimensional but large enough that there can be a significant spread in axial velocities. In CHRISTINE, it is assumed that the pitch factor has a Gaussian distribution and that the RMS width of the distribution can be specified (see Section 3). The initial conditions for the equations of motion are the following: particles are injected with a specified relativistic factor γ_0, pitch factor Θ, and entrance time $t(0)$. The number and distribution of injected particle entrance times are discussed later in this section.

CHRISTINE does not solve the quantity $t(z)$ directly using Eq. (9). Instead, it determines the phase relative to the n^{th} signal. This phase is defined as

$$\psi_n = \omega_n(z / v_{z0} - t) , \tag{11}$$

where v_{z0} is the initial axial velocity of a particle with pitch factor zero. It is evaluated taking voltage depression into account. The evolution of this phase is then given by

$$\frac{d\psi_n}{dz} = \omega_n(1 / v_{z0} - 1 / v_z) . \tag{12}$$

Introducing the phase ψ_n into the expression for the radiation field (Eq. (1a)) gives

$$\left.\frac{d\gamma}{dz}\right]_{rf} = Re \left\{ 2i \sum_n a_n(z)\, e_2(n,z)\, e^{i\psi_n} \right\} \tag{13}$$

for the contribution to the rate of change of γ due to the structure fields. In Eq. (13), the quantity $e_2(n,z)$ is defined as

$$e_2(n,z) = \frac{\langle \hat{z} \cdot \boldsymbol{e}_n \rangle_{beam}}{A_{eff,n}^{1/2}} \exp\left[i \int_0^z (k_{zn}(z') - \omega_n / v_{z0})\, dz' \right] , \tag{14}$$

where the angular bracket denotes average over the radial extent of the beam and over one axial period of the structure fields.

The above quantity also appears effectively in Eq. (7) for the complex field amplitude. To see this, we first represent the current density in the form of a sum over moving charge discs

$$j_z(r,z,t) = \sum_j \frac{v_{z,j}(t)\, \delta(z - z_j(t))}{\pi (r_{bo}^2 - r_{bi}^2)} \begin{Bmatrix} 0 , & r < r_{bi} \\ 1 , & r_{bi} < r < r_{bo} \\ 0 , & r > r_{bo} \end{Bmatrix} , \tag{15}$$

where the sum is over all the electrons. Equation (7) calls for an average over one spatial period of the structure and one temporal period of the fields. Due to the time periodicity of all quantities, this average may be evaluated by integration over the shaded region shown in Fig. 1.

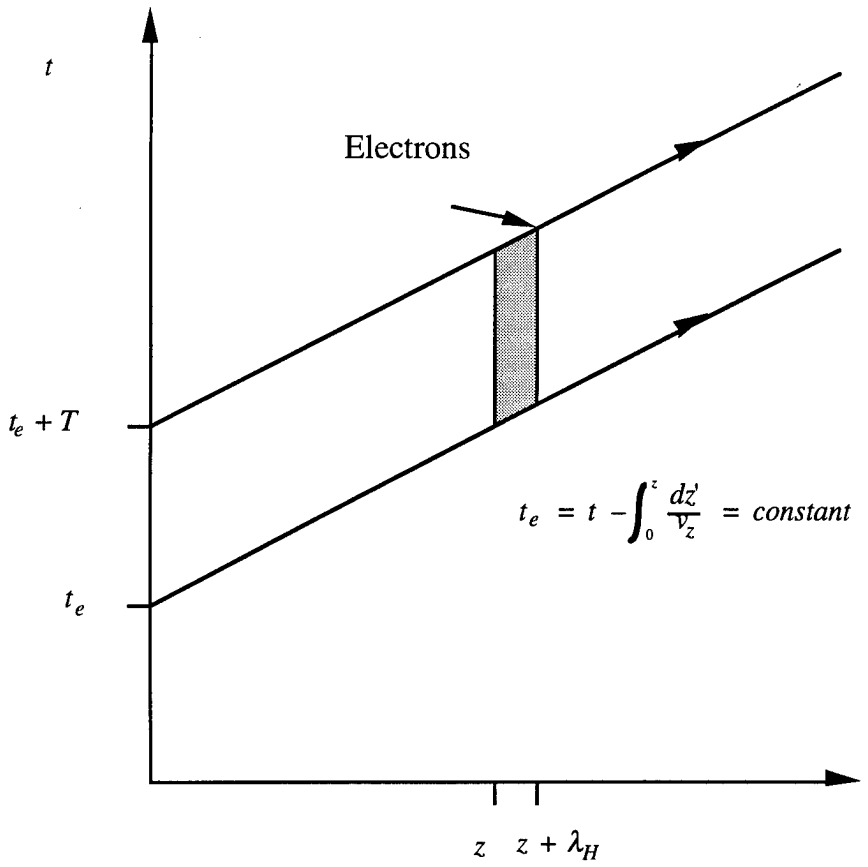

Fig. 1 — Characteristics in the t vs z plane for electron trajectories. The shaded region corresponds to one spatial period of the structure and one temporal period of the fields.

To evaluate the average, the shaded region, a parallelogram, is preferable to a rectangle, with upper and lower boundaries at fixed t because it contains the orbits of a group of electrons that all pass through both lateral boundaries. The average in Eq. (7) may be evaluated by first integrating over time:

$$\sum_j \int_z^{z+\lambda_H} \frac{dz\, e_n^*(x)\cdot\hat{z}}{\lambda_H} \int_t^{t+T} \frac{dt}{T} v_{z,j}(t)\, \delta(z - z_j(t))\, exp\,[-i(\int_0^z k_{zn}(z')\, dz' - \omega_n t)]$$

$$= \sum_{j'} \frac{1}{T} \int_z^{z+\lambda_H} \frac{dz\, e_n^*(x)\cdot\hat{z}}{\lambda_H}\, exp\,[-i(\int_0^z k_{zn}(z')\, dz' - \omega_n t_{j'})] \qquad (16)$$

where the sum over particles j' represents a sum over the group of particles entering the interaction region during one period of time T as depicted in Fig. 1 and $t_{j'}(z)$ is the time of flight for particle j' to the point z. The number of particles that will contribute to the sum is the number that entered during a time T, that is, TI/q, where I is the beam current. Now the integral over z can be carried out. Because the exponent is evaluated along a particle trajectory, it can be regarded as slowly varying over a distance given by the structure period λ_H. Thus, the average over z reduces to an average of the axial component of the structure field. Including the radial dependence of the current density implied by

the disc model, we see that Eq. (7) calls for precisely the same average of the structure fields as does the equation of motion. The result is that the average in Eq. (7) produces

$$\left(\frac{d}{dz} + \alpha_n(z)\right) a_n = \frac{2\pi i\, I}{I_A}\, e_2^*(n,z)\, \langle e^{-i\psi_n} \rangle , \tag{17}$$

where I is the total beam current and the angular brackets now signify average over particles entering the interaction region during the time interval T. Since the beam current enters in the form of a ratio I/I_A, the beam current and I_A can be evaluated in any system of units. In CHRISTINE, I is evaluated in amperes and $I_A = 1.7 \times 10^4$ amps. It is clear from Eqs. (13) and (15) that the relevant information concerning the structure fields is contained in the complex coupling function $e_2(n,z)$. The amplitude of this quantity is related to the axial impedance. In particular,

$$|e_2(n,z)|^2 = \frac{|\langle \vec{z} \cdot e_n \rangle_{beam}|^2}{A_{eff,n}} = \frac{K\, k_{zn}^2}{377\ \Omega} , \tag{18}$$

where K is the coupling impedance in ohms. The phase of the coupling function (Eq. (14)) is determined by the phase velocity of the structure fields.

The initial conditions on the phase ψ_n are determined by the distribution of particle entrance times. Basically, entrance times must be prescribed over the temporal period of the fields T. If the electron beam is unmodulated, the entrance times are uniformly distributed over this time interval. In the case of a premodulated beam with ballistic bunching, the initial entrance times are distributed according to the formula

$$t(z=0) = t' + \sum_{n=1} \frac{QB_n}{\omega_n} \cos\left(\omega_n t' + \Phi B_n\right) , \tag{19}$$

where the times t' are uniformly distributed over the interval T. In Eq. (19), QB_n and ΦB_n are the amplitude and phase of the modulation signal for frequency ω_n. In the case of premodulation at a single frequency ω_n, the ratio of average-to-peak beam current implied by Eq. (19) is $1 - |QB_n|$. Gated emission modulation presents two options. Either it is assumed that the current is on or off, giving a "top hat" dependence to the current on time, or it is assumed that the current has a "$\sin^2$" dependence on time. In these cases, the entrance times are uniformly distributed over a subinterval of the period of the bunching signal. The duration of the subinterval is specified by giving the ratio of the average current to the peak current. In the "$\sin^2$" case, each entering particle is given a weight between 0 and 2 according to the "$\sin^2$" distribution.

2.3 The Space Charge Field

This section describes the procedure for modeling the space charge electric field shown in Eq. (8). The effect of this field is to resist the formation of electron bunches and consequently to give rise to collective oscillations of the beam at a modified plasma frequency. The natural frequency of these oscillations depends on the beam density, its radial profile, and the configuration of the metallic structure surrounding the beam. We assume that the basic form of the field can be written as

$$\left\langle \hat{z}\cdot E_{sc}\right\rangle_{beam} = -\sum_n E_n \frac{4I}{\omega_n\left(r_{bo}^2 - r_{bi}^2\right)}\left\{i\left\langle e^{-i\psi_n}\right\rangle R_n' + c.c.\right\}, \tag{20}$$

where R_n' is an unknown coefficient that will be determined subsequently. Were this the only field acting on the particles, the linearized bunching factor would oscillate in time with an angular frequency ω_p, where

$$\omega_p^2 = \frac{4qIR'}{m\gamma_0^3 v_{z0}\left(r_{bo}^2 - r_{bi}^2\right)}. \tag{21}$$

This result is obtained by taking the small signal limit of Eqs. (8), (10), and (12) and assuming for simplicity that the beam is cold ($\Theta = 0$ in Eq. (10)). The factor R′ describes the reduction in the collective oscillation frequency accounting for the distribution of fields outside the beam.

CHRISTINE uses the sheath helix model to calculate the effects of the structure in the space charge field. This approach differs from others in that no attempt is made to separate fields into their electromagnetic and electrostatic components. This also allows unambiguous definition of the correct coefficient for the space charge field to include in the equation of motion. The space charge field that we seek has a time dependence similar to that of the structure fields (i.e., it is periodic in time with period T and thus includes frequencies belonging to the set ω_n). In general, more frequencies are needed to correctly model the space charge term than to model the structure fields. This is because, in the nonlinear regime, the bunched current density of the beam has a high harmonic content. Frequency ω_n is generally accompanied by spatial wave number ω_n/v_z. These spectral components of the current tend to excite modes of the structure over that range of frequencies where the dispersion relation of the structure is linear. However, as the excitation of the space charge field does not rely on resonance with the structure fields, the harmonic content of the current density produces appreciable space charge fields over a greater range of frequencies.

The approach taken by CHRISTINE is to assume that the beam current density is known and to then calculate the total ('structure' plus 'space charge') axial electric field at the beam that appears in response to the given current density. From the total field, one can then extract the appropriate factor R′. We assume that the form of the current density corresponds to an ensemble of moving annular discs oscillating in time with a frequency ω_n and an as yet unspecified wave number k_z. In order to connect the present calculation with the model of the current used in Eq. (7), we write

$$j_z(r,z,t) = \frac{I}{\pi\left(r_{bo}^2 - r_{bi}^2\right)} exp\left[i\left(k_z z - \omega_n t\right)\right]\left\langle e^{-i\psi}\right\rangle \begin{Bmatrix} 0, & r < r_{bi} \\ 1, & r_{bi} < r < r_{bo} \\ 0, & r > r_{bo} \end{Bmatrix} + c.c., \tag{22}$$

where r_{bo} and r_{bi} are the outer and inner radii of the beam discs, and the angular brackets represent the ensemble average over particles. Inserting Eq. (22) and its corresponding charge density perturbation determined by continuity into Maxwell's equations results in the following radial differential equation for the complex amplitude of the axial electric field with frequency ω_n and wavenumber k_z,

$$\left[\frac{\partial}{r\partial r}r\frac{\partial}{\partial r} - \kappa^2\right]\tilde{E}_z(r) = \kappa^2 \frac{4I}{\omega_n (r_{bo}^2 - r_{bi}^2)} \langle e^{-i\psi}\rangle \begin{Bmatrix} 0, & r < r_{bi} \\ 1, & r_{bi} < r < r_{bo} \\ 0, & r > r_{bo} \end{Bmatrix}, \tag{23}$$

where

$$\kappa^2 = k_z^2 - \frac{\omega^2}{c^2}. \tag{24}$$

We solve Eq. (23) for $r < r_H$, the radius of the sheath helix. In addition, we solve the similar (but homogeneous) equation for the axial magnetic field of the *TE* component of the radiation for $r < r_H$. Outside the helix (i.e., $r > r_H$), we solve similar homogeneous equations for the *TE* and *TM* components of the field, but assume that a dielectric with relative permitivity ε is present. The following boundary conditions are imposed: $E\theta(r)$ vanishes at $r = r_W > r_H$; $E_Z(r)$ vanishes at $r = r_V > r_H$ (where $r_W > r_V$), simulating the effect of vanes; and the components of the electric field parallel to the helix direction and the surface current perpendicular to the helix direction vanish at the helix. Finally, we average the axial electric field over the annular discs. The resulting expression for this averaged field is

$$\langle E_z \rangle_{beam} = -\frac{2i\omega_n}{c^2 D(k_z,\omega_n)} I\langle e^{-i\psi}\rangle [H]^2 - \frac{4iI}{\omega_n (r_{bo}^2 - r_{bi}^2)}\langle e^{-i\psi}\rangle R. \tag{25}$$

The quantity $D(k_Z,\omega_n)$ in the denominator of the first term in Eq. (25) is the vacuum dispersion function for the sheath helix:

$$D(k_z,\omega_n) = \frac{\omega_n^2 r_h^2}{c^2}\left[\frac{I_0'(\kappa r_h)}{\kappa r_h I_0(\kappa r_h)} - \frac{\varepsilon C_v'(\kappa_\varepsilon r_h)}{\kappa_\varepsilon r_h C_v(\kappa_\varepsilon r_h)}\right]$$

$$- \frac{1}{k_H^2 r_h^2}\left[\frac{\kappa r_h I_0(\kappa r_h)}{I_0'(\kappa r_h)} - \frac{\kappa_\varepsilon r_h D_w(\kappa_\varepsilon r_h)}{D_w'(\kappa_\varepsilon r_h)}\right], \tag{26}$$

where k_H is the helix wave number, D_W and C_V are linear combinations of Bessel functions

$$D_w(\kappa_\varepsilon r_h) = I_0(\kappa_\varepsilon r_h)K_0'(\kappa_\varepsilon r_w) - K_0(\kappa_\varepsilon r_h)I_0'(\kappa_\varepsilon r_w), \tag{27a}$$

$$C_v(\kappa_\varepsilon r_h) = I_0(\kappa_\varepsilon r_h)K_0(\kappa_\varepsilon r_v) - K_0(\kappa_\varepsilon r_h)I_0(\kappa_\varepsilon r_v), \tag{27b}$$

and

$$\kappa_\varepsilon^2 = k_z^2 - \frac{\omega^2\varepsilon}{c^2}. \tag{27c}$$

In Eq. (25), quantities H and R are defined as follows:

$$H = \frac{2\left[\,\kappa r_{bo} I_1(\kappa r_{bo}) - \kappa r_{bi} I_1(\kappa r_{bi})\,\right]}{\kappa^2 (r_{bo}^2 - r_{bi}^2)} \tag{28a}$$

and

$$R = 1 + \frac{2}{r_{bo}^2 - r_{bi}^2}\left\{ r I_1(\kappa r)\Big]_{r_{bi}}^{r_{bo}}\left[r_{bo} K_0'(\kappa r_{bo}) - \frac{K_0(\kappa r_h)}{I_0(\kappa r_h)} r I_1(\kappa r)\Big]_{r_{bi}}^{r_{bo}}\right]\right.$$

$$\left. - r_{bi} I_1(\kappa r_{bi}) r K_0'(\kappa r)\Big]_{r_{bi}}^{r_{bo}}\right\}. \tag{28b}$$

The first term in Eq. (25) is essentially the contribution of the structure field to the axial electric field at the beam, and the second term, involving R, is essentially the space charge field. The quantity R is the space charge reduction factor, and it is an interesting exercise in Bessel function identities to show that R vanishes as $r_{bi} \to r_{bo}$.

To determine the space charge field to be inserted in Eq. (8), we first write it in the form

$$\left\langle \hat{z} \cdot E_{sc} \right\rangle_{beam} = -\sum_n \frac{4I}{\omega_n \left(r_{bo}^2 - r_{bi}^2\right)} \left\{ i \left\langle e^{-i\Psi_n} \right\rangle R_n' + c.c. \right\}, \tag{29}$$

with R'_n to be determined. Assuming all fields vary as $exp(ik_z z)$, the total field implied by Eqs. (29) and (7) is

$$\left\langle \hat{z}\cdot E_{rf} + \hat{z}\cdot E_{sc} \right\rangle_{beam} = \sum_n \frac{2\pi i}{c\left(k_z - k_{zn}\right)} I \left\langle e^{-i\psi} \right\rangle \frac{|z\cdot e_n|^2}{A_{eff,n}} - \frac{4iI}{\omega_n \left(r_{bo}^2 - r_{bi}^2\right)} \left\langle e^{-i\Psi} \right\rangle R_n' + c.c.. \tag{30}$$

As can be seen, Eqs. (25) and (30) have similar behavior with respect to their dependence on k_z. They both diverge as $k_z \to k_{zn}$, where k_{zn} is the solution of the vacuum dispersion relation at frequency ω_n. We pick the space charge factor R_n' to give agreement between Eqs. (25) and (30) when both are expanded about $k_z = k_{zn}$. To lowest order, the coefficient of the singular term determines the impedance in the sheath helix model

$$\frac{K k_{zn}^2}{377\ \Omega} = \frac{|z\cdot e_n|^2}{A_{eff,n}} = -\left.\frac{\pi\, \omega_n [H]^2}{c\, \partial D(k_z, \omega_n)/\partial k_z}\right|_{k_{zn}}. \tag{31}$$

In next order, matching the coefficient of the constant term gives

$$R' = R - \frac{\omega_n^2\left(r_{bo}^2 - r_{bi}^2\right)D_s''}{4c^2\left(D_s'\right)^2}, \tag{32}$$

where

$$D_s' = \left.\frac{\partial\left(D/H^2\right)}{\partial k_z}\right|_{k_{zn}} \tag{33a}$$

and

$$D_s'' = \left.\frac{\partial D_s'}{\partial k_z}\right|_{k_{zn}}. \tag{33b}$$

The difference between R and R' can be interpreted as the effect of the sheath helix on the space charge reduction factor. In particular, if the helix is replaced by a conducting tube, no structure field can resonate with the beam, and the space charge reduction factor is simply R. With the helix present, some of the space charge field is able to penetrate outside the helix, and the reduction factor is modified.

Thus, the final equation of motion is

$$\frac{d\gamma}{dz} = \mathbf{Re}\left\{2i\sum_n a_n(z)e_2(n,z)e^{i\psi_n} - \frac{8Ii}{I_A\left(r_{bo}^2 - r_{bi}^2\right)}\sum_{n'}\frac{cR_{n'}'}{\omega_{n'}}e^{i\psi_{n'}}\left\langle e^{-i\psi_{n'}}\right\rangle\right\}$$

$$+ \frac{q}{mc^2}\left\langle \hat{z}\cdot\boldsymbol{E}_{dc}\right\rangle_{beam}, \tag{34}$$

where the separate sums over n and n' are over frequencies belonging to the set ω_n. In CHRISTINE, the number of frequencies kept to evaluate the space charge term is independent of the number kept to evaluate the structure fields. In particular, a range of frequencies is specified in the input list for the radiation field as is the number of space charge harmonics. In computing the space charge factor R_n' for each frequency harmonic, the code first checks to see if the frequency is in the range corresponding to the structure fields. If it is, the reduction factor is calculated according to Eq. (32). If the space charge harmonic frequency is out of the range specified for the structure fields, the reduction factor is taken to be just R and calculated for a spatial wave number $k_z = \omega_n/v_{z0}$.

3. NUMERICAL IMPLEMENTATION

This section outlines the numerical algorithm used to solve the basic equations. At various points in the discussion, physical variables from Section 2.2 are identified along with their FORTRAN equivalents in the program, which appear in brackets.

The main numerical calculation in the program is the integration of Eqs. (12), (15), and (34). This is done by a fourth order Runga-Kutta routine in subroutine 'rk'. This subroutine calls subroutine 'eqm' to evaluate the derivatives of each function. The following variables are integrated: the

complex field amplitude, $a_n(z)$, [as(nn,j)]; the relativistic factor, $\gamma(z)$, [gamma(kk)]; and the sine and cosine of the particle phase.

Because the complex exponential of the phase of each particle with respect to perturbations at each frequency is ultimately needed, i.e., $Z_n(z) = exp(-i\psi_n(z))$, [zc(nn,kk)], the following procedure is used. The phase is defined in Eq. (11), and its complex exponential is used in Eqs. (13), (15), and (34). The values of the Z_n are not independent because the frequencies are equally spaced. CHRISTINE calculates the sine [s(kk)] and cosine [c(kk)] of the phase for mode 0, which corresponds to the central frequency ω_0:

$$\frac{d \sin \psi_0}{dz} = \omega_0(1/v_{z0} - 1/v_z) \cos \psi_0 , \tag{35a}$$

$$\frac{d \cos \psi_0}{dz} = -\omega_0(1/v_{z0} - 1/v_z) \sin \psi_0 , \tag{35b}$$

and the sine [sd(kk)] and cosine [cd(kk)] of the phase corresponding to the difference frequency $\Delta\omega$:

$$\frac{d \sin \Delta\psi}{dz} = \Delta\omega (1/v_{z0} - 1/v_z) \cos \Delta\psi , \tag{36a}$$

$$\frac{d \cos \Delta\psi}{dz} = -\Delta\omega (1/v_{z0} - 1/v_z) \sin \Delta\psi . \tag{36b}$$

The following quantity is then formed in subroutine 'eqm,'

$$Z_n = e^{i\psi_n} = (\cos \psi_0 + i \sin \psi_0)(\cos \Delta\psi + i \sin \Delta\psi)^n . \tag{37}$$

In addition, the above quantity is raised to the m^{th} power to calculate the m^{th} harmonic of the space charge field for each frequency [zcm(nn,kk)],

$$Z_{n,m} = (Z_n)^m . \tag{38}$$

Some input parameters may overlap because the m^{th} harmonic of the space charge field for one frequency, $n1$, coincides with a higher frequency $n2$. This will occur if $m(\omega_0 + n1\ \Delta\omega) = \omega_0 + n1\ \Delta\omega$. Such possibilities are detected in subroutine 'initparam', where a table [iten(nn,nh)] is generated. If the element of the table for a particular n and m value is unity, then the corresponding $Z_{n,m}$ is kept in the space charge term. If the value is zero, the term is not kept.

3.1 Subroutines

The following paragraphs list and describe the functions of the various subroutines used in CHRISTINE.

3.1.1 Subroutine 'initparam'

This subroutine performs a number of preliminary calculations prior to integrating the wave equation and equations of motion. Among these are

1) introducing various physical constants,

2) determining the frequencies present in the RF spectrum,

3) determining the total number of particles,

4) invoking either subroutine 'S_HELIX' to calculate the phase velocity and impedance for the sheath helix model, or subroutine 'READ_DAT' to read in this information,

5) generating the axial grid and the interpolation factors for the profile of tapered quantities,

6) calculating the accelerating gradient [dvbeam(i)],

7) calculating the attenuation profile,

8) generating the distribution of electron velocities for a warm beam,

9) calculating the space charge coefficient for each frequency, and

10) initializing the amplitude of the injected signal at each frequency.

3.1.2 Subroutine 'expon'

This subroutine calculates the coupling factor $e_2(n,z)$ [e2(nn,j)], which is defined in Eq. (14). It requires the phase velocity and coupling impedance for each frequency.

3.1.3 Subroutine 'phases'

This subroutine initializes the phases of the entering simulation particles as detailed in Section 2. For a gated emission, weights are also given to the entering particles to describe the time dependence of the beam current.

3.1.4 Subroutine 'rk'

This subroutine, the Runga-Kutta integrator, integrates the equations of motion and the wave equation. It invokes subroutine 'eqm' to calculate the rate of change of each quantity to be varied. In addition, this subroutine tabulates and writes the particle data to files. This information is discussed more completely in Section 4.1.

3.1.5 Subroutine 'srs'

This subroutine invokes subroutine 'rk' and it tracks the power balance.

3.1.6 Subroutine 'eqm'

This subroutine computes the right-hand side of Eqs. (15), (34), (35), (37), and (38). It is invoked by subroutine 'rk'.

3.1.7 Subroutine 'S_HELIX'

This subroutine solves the dispersion relation for the sheath helix model by using Newton's method. It also determines the coupling impedance and space charge correction factor caused by fields outside the helix.

3.1.8 Subroutine 'READ_DAT'

This subroutine reads in the parameters of the structure as an alternative to using the sheath helix model. Section 4 describes the format for inputting data.

3.2 Input Namelists

Input for CHRISTINE is provided through 'tiniS.nml' (Table 1), a file that contains a sample set of namelists corresponding to a specific research tube. This input file is used as a basis for the set of example runs presented in Section 4. The various namelists are summarized in the following paragraphs.

Table 1 — CHRISTINE Input File 'tiniS.nml'

```
curbeam - beam current (in Amps)
tht_sprd - maximum injection angle in degrees
        controls effective axial velocity spread
vbeam - beam voltage (in Volts)
rbo     - outer beam radius (in cm)
rbi     - inner beam radius (in cm)
shotn    - shot noise in beam (shotn = 1. is the nominal value)
dc_sc   - if true, DC space charge depression is applied to beam energy

 $beam
   curbeam  = .17,
   tht_sprd  = 0.,
   vbeam   = 2.84e3,
   rbo   = .036,
   rbi   = .03,
   shotn   = 0.,
   dc-sc =.false.
 $end

delfreq     - resolution in frequency
freq0      - central frequency
freq_max    - maximum frequency
freq_min    - minimum frequency
pow_in     - array of input powers [watts]
phase_in    - array of input phases in radians
QB       - array of prebunching factors
Phase-B     - array of prebunching phases
gated_I     - if true, modulation of current
```

Table 1 — CHRISTINE input file 'tiniS.nml' (continued)

```
sin_2      - if true, sin^2 time dependence, otherwise top hat
AveI_pkI   - average current divided by peak current

 $rad
    freq0 = 5.e9,
    delfreq = 5.e9,
    freq_max = 5.e9,
    freq_min = 5.e9,
    pow_in = 2.4e-03,
    phase_in = 0.,
    QB =.0,
    phase_B = 0.,
    gated_I = .false.,
    sin_2 = .true.,
    AveI_pkI = .60,
$end
nz        - number of axial points
na0       - number of velocity angles
fnt0      - number of entrance times per mode
np0       - number of phases
nsc       - number of space charge harmonics


$num
    nz   = 300,
    na0  = 1,
    fnt0  = 1.5,
    np0  = 137,
    nsc  = 1,
 $end

zint      - interaction length
zr(i)     - axial points where parameters are specified.
        All quantities are piecewise continuous between
        these points, the first point should be zero and
        the last should be greater than or equal to zint.
dvbeam(i)  - acceleration potential
use_sh     - if true, uses sheath helix model

 $struct
   zint   = 9.5758,
   zr     = 0., 10.,
   dvbeam   = 2*0.
   use_sh   = .true.,
 $end

RH(i)     - array of helix radii
H_LMDA(i)  - array of helix periods
RW(i)     - array of wall radii
EPS_R(i)   - array of dielectric constants
RV(i)     - array of vane radii (if no vanes, set this equal to RW)
use_cor    - if true, adds correction to space charge term
```

Table 1 — CHRISTINE input file 'tiniS.nml' (continued)

```
   $helix_par
    RH = 2*.12446,
    H_LMDA = 2*.080137,
    RW = 2*.2794,
    EPS_R =2*1.75,
    RV =  2*.2794,
    use_cor = .false.
 $end

za(i)     - array of z points for specification of attenuation
att(i)    - array of attenuation
dB_cm     - if true, att in dB/cm, otherwise dB/wavelength
f_scale   - attenuation proportional to (f/freq0)**f_scale

$loss_par
    za = 0.,10.,
    att = 2*0.,
    dB_cm = .true.,
    f_scale = 0.
 $end

nt_plot   - number of times for beta vs z plots
ps_z      - array of axial positions for phase space plots

 $ps_plot
    nt_plot = 3,
    ps_z = 5.,7.,9.,
 $end

To read in structure properties
npts      - number of data points
f_in(i)   - array of frequencies
bp_in(i)  - array of phase velocities
z_in(i)   - array of impedances
RH_eff    - effective helix radius for calculating space charge
fract_bp  - modify above phase velocities at points zr(i)
fract_Z   - modify above impedances at points zr(i)
use_dat   - if true, read in parameters from my.bp and my.zc

 $dis_dat
    npts = 15,
    f_in =
 1.e09,2.e09,3.e09,4.e09,5.e09,6.e09,7.e09,8.e09,9.e09,10.e09,11.e09,12.e09,13.e09,14e09,15.e09,
    bp_in =
0.10790,0.10530,0.10160,0.097790,0.094480,0.092000,0.090270,0.089090,0.088300,0.087770,0.0
87400,0.087140,0.086960,0.086840,0.086750
    z_in =
236.40,212.30,172.00,123.20,78.920,47.030,27.090,15.430,8.8040,5.0490,2.9170,1.6970,0.99390,0
.58570,0.34710
    fract_bp =2*1.,.89,.79
    fract_Z = 2*1.,.84,.68
    RH_eff = .12446,
```

Table 1 — CHRISTINE input file 'tiniS.nml' (continued)

```
use_data = .true.,
 $end

scan_p     - parameter scanning activated if .true.
n_harm     - number of harmonics in radiation field
        ( freq_max = (n_harm+1)*freq0 )

varX     - variable to be scanned
varY     - variable to be scanned
       possibilities are:

       curbeam
       vbeam

tht_sprd
       rbo
       rbi
       freq0
       pow_in (1)
       pow_in (2)
       phase_in (1)
       phase_in (2)
       QB
       AveI_pkI

nx       - number of values of varX
ny       - number of values of varY
varX_min    - minimum value of varX
varX_max    - maximum value of varX
varY_min    - minimum value of varY
varY_max    - maximum value of varY
log_X  - if true, varX scanned logarithmically
log_Y  - if true, varY scanned logarithmically

 $scan
   scan_p = .true.
   n_harm = 0,
   varX = 'vbeam',
   nx = 25,
   varX_min = 2.0e3,
   varX_max = 3.5e3,
   log_X  =.false.
   varY = 'freq0',
   ny =1,
   varY_min = 5.e9,
   varY_max = 5.e9,
   log_Y  =.false.
 $end
```

3.2.1 Namelist - beam

These are the physical parameters of the beam. For a cold beam, 'tht_sprd' = 0. To simulate a warm beam, set 'tht_sprd' to the RMS width $\Delta\theta$ (in degrees) of the distribution of injected angles of the beam electrons. CHRISTINE assumes the distribution is Gaussian:

$$P(\theta) = \frac{2\theta}{(\Delta\theta)^2} \exp\left(-\frac{\theta^2}{(\Delta\theta)^2}\right). \tag{39}$$

The number of injection angles used is controlled by the variable 'na0' appearing in namelist 'num'. Injection angles are chosen so that the particles have equal weights (i.e., the values of the cumulative distribution function are equally spaced):

$$\left(\frac{\theta_i}{\Delta\theta}\right)^2 = ln\left(\frac{na0}{na0 + 1/2 - i}\right), \; i = 1, na0 . \tag{40}$$

The beam is assumed to be annular with inner and outer radii 'rbi' and 'rbo' such that 'rbi' < 0.95 'rbo'. Otherwise, the space charge term is not calculated accurately. For a solid beam, set 'rbi' to 0.

The variable 'shotn' controls the noise on the injected beam. Basically, each injected particle is given a small random component to its weight. With *'shotn' = 0*, the random component is zero and the simulation is noiseless. With *'shotn' = 1*, the random component is calculated to correspond to the shot noise produced by uncorrelated electrons at the specified beam current. This is probably an overestimate of the noise level produced by space charge limited guns. The correct value of noise depends on features of the gun not modeled in CHRISTINE.

The beam energy will be depressed by the DC space charge potential when the logical variable 'dc_sc' is set to *.true.*. The amount of depression is given by the formula

$$\frac{qV}{mc^2} = \frac{2Ic}{I_a v_{zo}}\left\{ln\frac{r_H}{r_{bo}} + \frac{1}{4} - \frac{r_{bi}^2}{2\left(r_{bo}^2 - r_{bi}^2\right)}\left[1 + \frac{r_{bi}^2}{r_{bo}^2 - r_{bi}^2} ln\left(\frac{r_{bi}^2}{r_{bo}^2}\right)\right]\right\}, \tag{41}$$

where r_H is the helix radius, which is assumed to be at ground potential.

3.2.2 Namelist - rad

This namelist specifies aspects of the radiation. The first four variables determine the properties of the spectrum of the RF fields. The spectrum is assumed to consist of frequencies spaced equally about 'freq0' by an amount 'delfreq'. The quantity 'freq0' should be an integer multiple of 'delfreq'. If it is not, the code adjusts the value of 'delfreq' so that it is. The spectrum then consists of all frequencies between 'freq_min' and 'freq_max' that differ from 'freq0' by an integer multiple (positive or negative) of 'delfreq'. Arrays 'pow_in', 'phase_in', 'QB', and 'phase_B' control the signal injected into the interaction regions. The elements of the array correspond to the frequencies in the spectrum going from smallest to largest. Thus, some care needs to be exercised in assigning numerical values to these variables. One has to first compute which frequencies will be present in the simulation based on the values of 'freq0', 'delfreq', 'freq_min', and 'freq_max', and then enter the numerical values for the signal parameters in the correct order. The definition of QB

and its phase 'phase_B' can be found in Eq. (19). The phases 'phase_in' and 'phase_B' are defined with respect to some arbitrary reference time. In principle, only the relative phases of the input signals affect the output signal. However, as discussed in the next paragraph, one of the diagnostics is keyed to the reference time.

An alternate way of exciting a signal in the structure is to modulate the beam current. This is done by using the logical input *gated_I = .true.*. With this option, only **one frequency** and possibly its harmonics can be used in the simulation. In other words, 'delfreq' is set equal to 'freq0'. The temporal shape of the modulated current is controlled by the logical variable 'sin_2'. With *sin_2 = .true.*, the current pulse has a sine-squared temporal waveform, otherwise it is a top hat. The duration of the current pulse is controlled by the variable 'AveI_pkI', which is the ratio of the average current to the peak current in the pulse. The variable 'curbeam' always represents the average current.

3.2.3 Namelist - num

This namelist controls the basic numerical parameters in the integration scheme in CHRISTINE. The number of axial points required, 'nz', depends on the number of exponentiations of the signal as it passes through the interaction region. A value of 200 is probably a safe minimum; if a much larger value is required, the results should be tested for significant change. The number of injected particles is controlled by the variables 'na0', 'fnt0', and 'np0'. As mentioned, 'na0' controls the number of injected pitch angle groups. When simulating a cold beam, this number should be one. Otherwise, a higher number is needed. Again, the number needed depends on many factors and the best way to judge is to test the sensitivity of the results to varying the number. The variable 'fnt0' controls the number of injected particles when the spectrum has multiple frequencies. If there are 'nw' frequency components in the spectrum, the number of injected particles is roughly 'na0*fnt0*nw*np0'. For a single frequency, the number is simply 'na0*np0'. This peculiar way of specifying the number of particles is designed to automatically adjust the number of particles to maintain high accuracy as the parameters of the RF spectrum are changed. The setting *fnt0 = 1.5* should minimize the amount of aliasing in calculating the source term for each component of the spectrum. However, this number may have to be increased if the spectrum is particularly asymmetric about 'freq0'. The variable 'np0' controls the basic number of entrance phases. Its size depends on the number of space charge harmonics that are believed to be important. At a minimum, 'np0' should be on the order of 20 (it's better to use prime numbers). Also, approximately 10 entrance phases should be alloted to each space charge harmonic. The number of space charge harmonics is given by the variable 'nsc'. If this is set to zero, the space charge field is not included.

3.2.4 Namelist - struct

This namelist gives some general parameters of the structure. Array 'zr' is an ordered set of axial positions where the parameters of the structure are to be specified. The first element must be zero and the last must be **greater than or equal to** the length of the structure, which is given by variable 'zint'. Various axially dependent parameters will be defined later on this set of points. Typically, it is assumed that quantities vary piecewise linearly between points. For example, 'dvbeam' is a vector of voltages defined for the points 'zr'. (Again, the first element should be zero.) The values of 'dvbeam' and 'zr' determine the piecewise linear accelerating potential throughout the interaction region. This potential can act to accelerate particles to improve efficiency similar to the effect of tapering the structure period. To deactivate this potential, set all elements of 'dvbeam' to zero.

The number of entries for the parameters 'zr' and 'dvbeam' should not exceed by more than one the value of the integer parameter 'nzpts' (this parameter is declared in each of the code's subroutines). That is, arrays 'zr' and 'dvbeam' are declared to have 'nzpts+1' elements. The same

will be true for a number of variables in namelists 'helix_par' and 'dis_dat'. Applications that need many axial points to specify the profiles of the structure parameters require **going into the code and changing** parameter 'nzpts' in each place that it appears. When fewer than 'nzpts+1' points are required to specify the profiles, it is usually safe to input fewer than that many values for the relevant arrays. This is illustrated in Section 4.

Abrupt changes in parameters can be modeled by assigning the same axial position to two successive elements of 'zr', and then assigning two different values of the relevant parameter to the appropriate array. The code will place the values at two adjacent points on the axial grid. It is not recommended that you do this for the accelerating potential 'dvbeam' as that would describe an infinite accelerating field.

The logical variable 'use_sh' controls the way the dispersive properties of the structure are input to the code. If *use_sh = .true.*, a sheath helix model is assumed and the parameters for the sheath helix are given in namelist 'helix_par'. If *use_sh = .false.*, the impedance, phase velocity, and equivalent helix radius (required to calculate the space charge field) are read from namelist 'dis_dat' or read in from files 'my.bp' and 'my.zc'. This is discussed in more detail in the example described in Section 4.8.

3.2.5 Namelist - helix_par

This namelist gives arrays of the parameters of the sheath helix; 'RH' is the helix radius in cm, 'H_LMDA' is the helix period in cm, 'RW' is the wall radius in cm, 'EPS_R' describes the effective dielectric constant of the helix supports, and 'RV' is the effective vane radius in cm. If there are no vanes, 'RV' is set equal to wall radius 'RW'. The various values are defined for the set of points 'zr' given in namelist 'struct'. The number of entries for each parameter should not exceed by more than one the value of the integer parameter 'nzpts'. That is, the code expects to read in no more than 'nzpts+1' values for each of the following arrays: 'RH', 'H_LMDA', 'RW', 'EPS_R', and 'RV'. The logical 'use_cor' controls the form of the space charge term in the equation of motion. If *use_cor = .false.*, the space charge term is calculated with the assumption that the helix is a perfectly conducting tube; otherwise, the correction to the space charge term accounting for fields outside the helix, as calculated in Section 2.3, is included.

3.2.6 Namelist - loss_par

This namelist allows one to specify the axial dependence of the attenuation in the structure. Here, 'za' is an array analogous to 'zr', and 'att' is an array of values of attenuation. The profile of attenuation is taken to be piecewise linear between the points 'za'. The maximum allowed length of these arrays is controlled by the parameter 'nzapts' defined in subroutines 'main' and 'initparam'. The values of attenuation may be entered either in dB/cm or in dB/$\lambda = k_{zn}$ dB/(2π) (that is, dB per axial wavelength). To enter the data in dB/cm, set the logical 'dB_cm' to true. The variable 'f_scale' allows for flexibility in specifying the frequency dependence of the attenuation. With 'f_scale' = 0., the frequency dependence of the attenuation is as follows. When entering in dB/cm, all signal frequencies will have the same rate of attenuation. If the logical 'dB_cm' is set to false, then each signal frequency will have the same rate of attenuation as measured in dB/λ. However, since different signal frequencies have different axial wavelengths, the resulting rates of attenuation in dB/cm for each signal frequency will be different. With 'f_scale' not equal to 0, an additional frequency dependence is imposed on the attenuation. Specifically, the attenuation for each frequency f is multiplied by a factor $(f/freq0)^{f\_scale}$.

3.2.7 Namelist - ps_plot

This namelist controls some of the output from CHRISTINE, in particular information about the coordinates of particles at various times and points in the the interaction region. Two types of data files for making plots are generated: snapshots of the positions and velocities of particles at given times, and phase space information, namely the velocities and phases of particles at specified axial positions. These files are not written if the program is in the parameter scan mode (*scan_p = .true.*) The variable 'nt_plot' specifies the number of snapshot files to be written. (If *nt_plot = 0.*, then no snapshot files are written.) As the fields are assumed to be time periodic, snapshots of the particle positions and velocities are time periodic as well. Thus, it does not make sense to specify an absolute value of time at which to make a snap shot. Instead, one specifies the number of snapshots, and these are taken at times distributed uniformly over the period of the fields. If only one frequency is present, 'freq0', the period of the fields is the reciprocal of this frequency. Otherwise, the period is the reciprocal of the frequency spacing 'delfreq'. The files are written out and given the names 'bvsz_XXpYY', where YY is the number of snapshots ('nt_plot') and XX is an integer between 1 and YY indicating the time interval. The first of these plots corresponds to the reference time relative to which the phases of the input signals are defined. Equation (1) presents the convention for defining the phases of the signal field.

The array of variables 'ps_z' gives the axial positions at which phase space data are written. If a single frequency is present, the phase space consists of the particle velocity and the phase ψ_0. If multiple frequencies are present, the phase space is the particle velocity and the phase $\Delta\psi$. The phase space files are given the names 'PS_ZZ', where ZZ is the index corresponding to the element of array 'ps_z'.

3.2.8 Namelist - dis_dat

This namelist allows one to enter directly the relevant parameters for simulating a structure that is not well described by a sheath helix, or one for which measured data are available. The variables 'npts', 'f_in', 'bp_in', and 'z_in' determine the dispersive properties of the structure. The latter three quantities are arrays with 'ntpts' elements. Array 'f_in' is a set of frequencies that spans the range 'freq_min' to 'freq_max'. Array 'bp_in' is the set of phase velocities, normalized to the speed of light, corresponding to the frequencies in 'f_in'. Array 'z_in' is the corresponding set of coupling impedances. CHRISTINE uses these arrays to interpolate the appropriate values of phase velocity and impedance for the set of frequencies in the simulation.

If the structure is tapered, namelist 'dis_dat' provides a quick and dirty way to enter the tapering profile. This is through arrays 'fract_bp' and 'fract_Z'. These arrays allow you to modify the data entered in arrays 'bp_in', and 'z_in'. For example, 'fract_bp' is an array of factors corresponding to the set of axial points defined in 'zr'. The axially dependent phase velocities are then defined by multiplying the value of 'bp_in' corresponding to the frequency of interest by the value of 'fract_bp' corresponding to the axial position of interest. Similarly, the axially dependent impedance is defined as the product of 'z_in' and 'fract_Z'. This procedure is admittedly crude because varying a parameter of the structure does not result in the phase velocity or impedance of all frequencies changing by the same factor. However, it does allow for a treatment of tapered profiles when all the relevant information is not available.

A more satisfactory way to input tapered structure data is to set the logical 'use_data' to true. The code then looks for files named 'my.bp' and 'my.zc' containing columns of numbers describing the phase velocities and impedances of the different sections of the structure. In this case the frequency,

phase velocity, and impedance data in the name list are ignored. The format of the files 'my.bp' and 'my.zc' should be as follows. There should be 'npts' rows of data. The first column of each file should contain the frequencies replacing 'f_in'. This column should be the same in both files. The next columns in each file contain the phase velocities or impedances for each of the points defined by 'zr' in the structure. The code first examines 'zr' to determine how many columns to read. It then reads in the data via an unformatted read statement. Thus, tabs or spaces may be used to delineate columns. An example is given in Section 4.8.

3.2.9 Namelist - scan

The elements of this namelist control the parameter scanning feature of CHRISTINE. To activate the scanning feature, set 'scan_p' to .true. The variables that can be scanned are listed in the comment field of the input file. CHRISTINE will then perform a matrix of runs corresponding to a scan over the variables 'varX' and 'varY'. The values assigned to scanned variables then override those specified in the other namelists. Additionally, other features of the code are overridden when it is in the scanning mode. First, one **cannot do general multifrequency simulations** in the scanning mode. Instead, one is restricted to single frequency, or multifrequency with harmonics-only simulations. Specifically, in scanning mode, variables 'delfreq' and 'freq_min' are set equal to the relevant value of 'freq0'. Variable 'freq_max' is set equal to the product of 'freq0' and 'n_harm'+1, where 'n_harm' is the number of harmonics to be retained. Thus, to simulate a single frequency, set 'n_harm' to 0. The values that the variable 'varX' will take on are controlled by the input parameters 'nx', 'varX_min', varX_max', and 'log_X'. Basically, 'varX' will assume 'nx' values between 'varX_min' and 'varX_max', inclusive. If 'nx' = 1, only the minimum value is simulated. If 'log_X' is .false., the values of 'varX' will be incremented linearly between the two limits. With 'log_X' set to .true., the logarithm of 'varX' is incremented linearly. Similar rules apply to 'varY'.

In the scanning mode, CHRISTINE produces the following output files: 'gain', 'efficiency', and 'P_out.N'. (Files such as 'axial' and those containing particle trajectory data are not printed out when the code is in the parameter scanning mode.) Each of the output files contains a table where the rows correspond to the different values of 'VarX' and the columns correspond to the different values of 'varY'. The file 'gain' contains the magnitude and phase of the gain of the fundamental frequency signal for each of the input parameters. The files 'P_out.N' contain the output power in the 'N th' signal frequency, where N = 1 is the fundamental, N = 2 the harmonic, and so on. The file 'efficiency' contains the efficiency of beam-to-output power conversion based on the output power in the fundamental frequency.

4. SAMPLE RUNS

This section presents several illustrations of the code's features by providing sample namelist files. The physical parameters used are based on a specific research tube. The following examples are presented:

1. Sheath helix modeling
2. Phase space plots
3. Scanning parameters
4. Space charge
5. Harmonic generation
6. Multifrequency simulations
7. Tapering and attenuation
8. Importing dispersion and coupling impedance data.

The first several examples use the input file shown in Table 1.

4.1 Sheath Helix Modeling

The sheath helix model is activated by setting the logical variable 'use_sh' to true in namelist 'struct'. The parameters of the helix are then entered in namelist 'helix_par'. (If 'use_sh' is set to false, then none of the information in 'helix_par' is used. Instead, information in 'dis_dat' is used. This is discussed in Section 4.8.) For this example, an untapered helix with the following dimensions is specified: helix radius = 0.12446 cm, helix period = 0.080137 cm, wall radius = 0.2794 cm, vane radius = 0.2794 cm, and effective dielectric constant of helix supports = 1.75. Note that in this case, the wall radius and vane radius are the same. This corresponds to the case with no vanes. Note also that two entries appear for each parameter (e.g., *RH = 2*.12446*). This is because the axial profile of the corresponding variable is taken to be a piecewise linear function between successive values of the elements of array 'zr' appearing in namelist 'struct'. In the current example, the first two elements of 'zr' are 0.0 and 10.0. As this second number is the first to exceed the length of the interaction region (*zint = 9.5758*), all subsequent elements of 'zr' are unimportant and the axial profile of various functions is taken to be piecewise linear for z between 0.0 cm and 10.0 cm. In order to represent a constant, one must specify the two values of the parameters corresponding to the points zr = 0 and zr = 10 to be the same.

The characteristics of the RF spectrum are controlled by namelist 'rad'. The present case prescribes a 5 GHz, single frequency run. The minimum and maximum frequencies ('freq_min' and 'freq_max') are the same as the central frequency ('freq0') and the frequency separation ('delfreq'). Examples of multifrequency runs are given in Section 4.6. The input power of the signal ('pow_in') is 2.4×10^{-3}W, and the phase (phase_in) is zero radians. As discussed in Section 2.2, the phase is defined with respect to a reference time to which the particle diagnostics discussed in Section 4.2 are keyed. The ballistic prebunching amplitude and phase are both zero, and the current is ungated (i.e., *gated_I = .false.*).

Numerical parameters are controlled by namelist 'num' (Section 3.2.3). Sheath helix modeling offers a total of 137 entrance times, which is probably many more than is necessary. Only one space charge harmonic is included in the simulation. The effect of varying the number of space charge harmonics is discussed in Section 4.4.

Running the code produces the following output files: 'dispersion', 'impedance', 'axial', 'P_out', 'bvsz_01p03', 'bvsz_02p03', 'bvsz_03p03', 'PS.01', 'PS.02', and 'PS.03'. Files 'dispersion' and 'impedance' contain tables of the normalized phase velocity and coupling impedance, respectively, calculated in the sheath helix approximation for the frequency spectrum prescribed in namelist 'rad'. This example offers only one frequency (5 GHz). CHRISTINE tabulates two phase velocities and coupling impedances for each frequency, corresponding to the values of the relevant quantity at the set of axial points contained in 'zr'. In this example, therefore, two identical values are tabulated for each quantity. The example described in Section 4.6 generates a more interesting table.

File 'axial' contains a table of the axial profiles of the average beam energy and the power in each frequency component of the RF signal. Figure 2 plots the data for the present run. File 'P_out' contains a table of output power vs frequency. This information is already present in the last line of the file 'axial', and thus, is redundant. However, when doing multifrequency simulations, use of this table provides a convenient way of displaying the output spectrum.

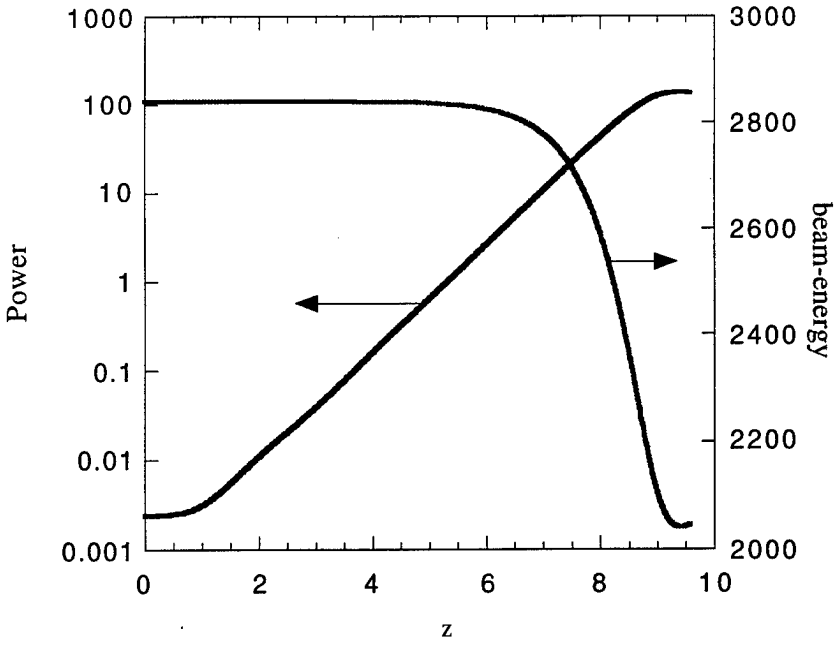

Fig. 2 — File 'axial': power and average beam energy vs z

Files 'bvsz_01p03', 'bvsz_02p03', 'bvsz_03p03', 'PS.01', 'PS.02', and 'PS.03' display information about the trajectories of individual particles and are discussed in Section 4.2.

4.2 Phase Space Plots

Namelist 'ps_plot' controls the output of the files containing data on the particle trajectories. The parameter 'nt_plot' gives the number of files containing the axial position and normalized axial velocity coordinates of particles at a fixed time. This example produces three such files: 'bvsz_01p03', 'bvsz_02p03', and 'bvsz_03p03'. The first of these gives the coordinates at a time corresponding to the reference time (keyed to the phase of the input signal) and the second and third give the coordinates of the particles one third and two thirds of a period of the signal later, respectively. Figure 3 is a scatter plot of the data in 'bvsz_01p03'.

Files 'PS.01', 'PS.02', and 'PS.03' contain phase space data (i.e., tables of phase and normalized axial velocity of particles at specific values of axial position). The axial positions are controlled by the elements of array 'ps_z'. The files are numbered consecutively corresponding to these elements. Figure 4, a plot of the phase space coordinates contained in 'PS.03' corresponding to z = 9 cm, clearly shows the saturation of the amplifier caused by phase trapping.

Particle trajectory data are not printed out when the code is in the parameter scanning mode, which is illustrated in Section 4.3.

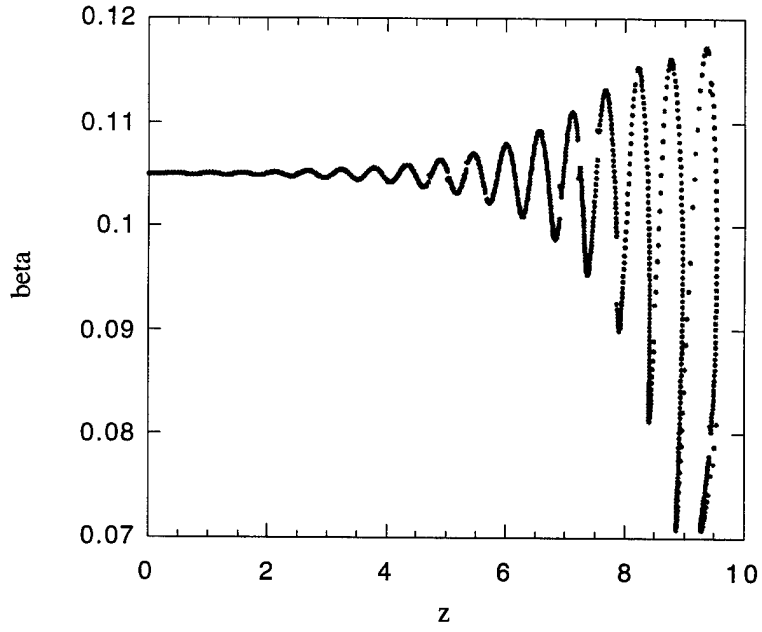

Fig. 3 — File 'bvsz_10p03': normalized velocity vs z at the reference time

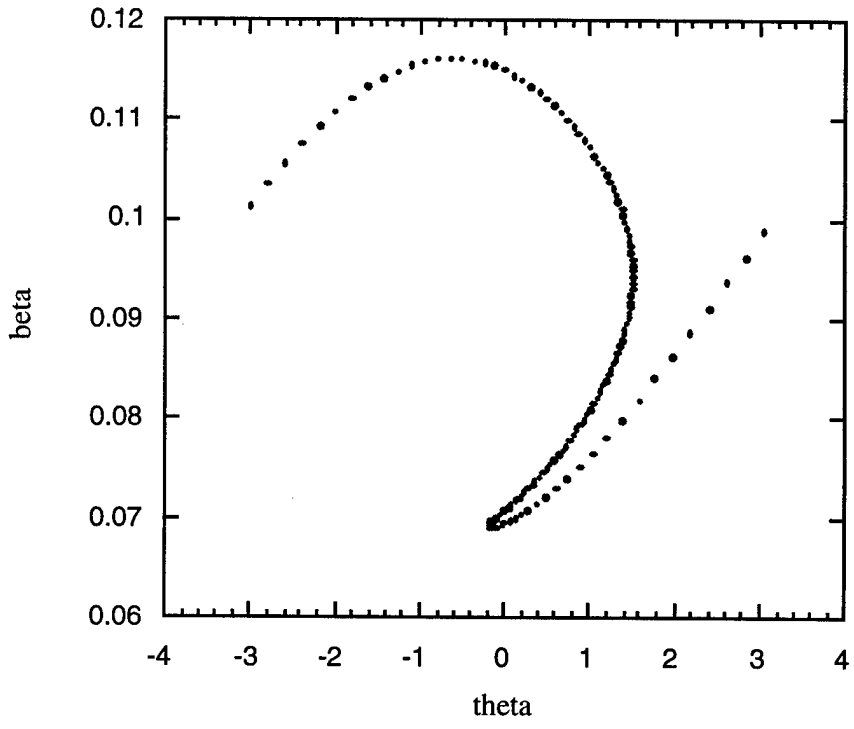

Fig. 4 — File 'PS_03': normalized velocity vs phase for all particles at z = 9.0 cm

4.3 Scanning Parameters

The preceding example produced data for a single set of input parameters. Often it is desired to vary parameters and plot the results vs the parameter that is varied. This feature is controlled in CHRISTINE by namelist 'scan'. To activate the parameter scanning feature, the logical parameter 'scan_p' is set to true. A sample scan namelist is shown below.

```
$scan
   scan_p = .true.
   n_harm = 0,
   varX = 'vbeam',
   nx = 50,
   varX_min = 2.0e3,
   varX_max = 4.0e3,
   log_X = .false.
   varY = 'freq0',
   ny = 2,
   varY_min = 5.e9,
   varY_max = 6.e9,
   log_Y = .false.
 $end
```

This namelist prescribes that two variables, 'vbeam' and 'freq0', are to be varied. There will be 50 different values of 'vbeam' between 2.0 kV and 3.0 kV, and two values of 'freq0' between, in this example, 5 GHz and 6 GHz. The code will thus simulate the operation of the device for 100 different sets of parameters.

Running the code with the sample namelists produces the following output files: 'gain', 'efficiency', and 'P_out.1'. (Files such as 'axial' and those containing particle trajectory data are not printed out when the code is in the parameter scanning mode.) Each of these contains a table where the rows correspond to the different values of 'VarX' (in this case 'vbeam') and the columns correspond to the different values of 'VarY' (in this case 'freq0'). File 'gain' contains the magnitude and phase of the gain of the fundamental frequency signal for each of the input parameters. File 'P_out.1' contains the output power in the fundamental frequency, and 'efficiency' contains the efficiency of the beam-to-energy power conversion based on the output power in the fundamental frequency. If harmonics are included by setting 'n_harm' to an integer different from zero, then the output power in each harmonic is printed in file 'P_out.N', where N is an integer labeling the frequency of the corresponding signal, 1 implies the fundamental, 2 the second harmonic, and so on. Figure 5 plots file 'P_out.1'.

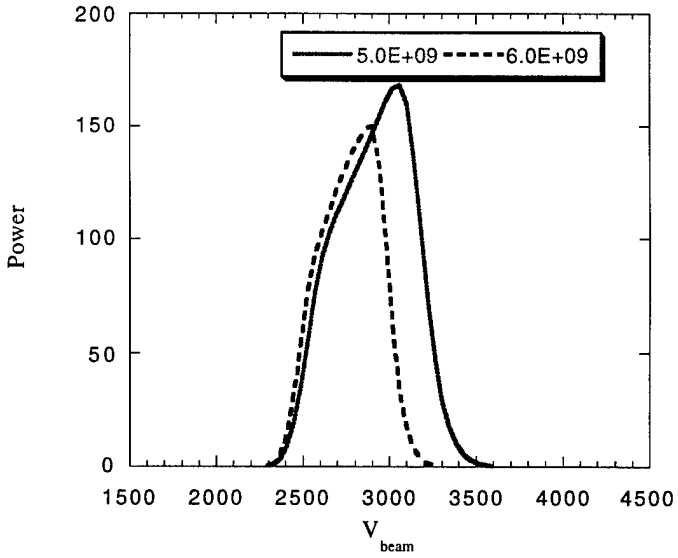

Fig. 5 — File 'P_out.1': output power vs beam voltage for two values of the input frequency

4.4 Space Charge

The number of space charge harmonics is controlled by parameter 'nsc' in namelist 'num'. As discussed in Section 4.1, the space charge field can have a strong temporal harmonic content even if the RF signal field is relatively pure. Figure 6 illustrates this by displaying the results of a number of parameter scan runs with differing numbers of space charge harmonics. (Parameter 'nsc' cannot be scanned automatically, so this plot is made by collecting data from a number of runs.) Generally speaking, as the number of space charge harmonics increases, so does the number of particles 'np0'. In this example, all runs were conducted with 'np0' = 137. Additionally, the sheath helix correction to the space charge field was not activated (i.e., *use_cor* = *.false.*).

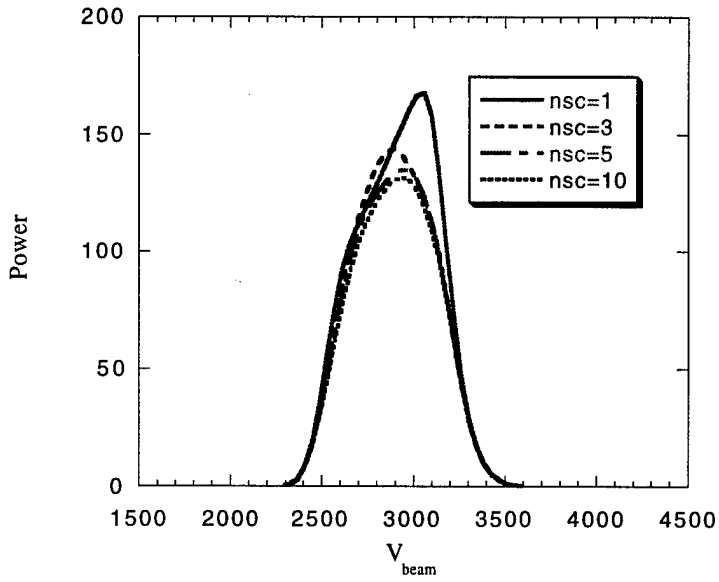

Fig. 6 — Output power vs beam voltage for 'freq0' = 5.0 GHz and several values of 'nsc'

The plot shows that between five and ten space charge harmonics are required to obtain a converged result. This is because the output has saturated and the bunched beam current has a high harmonic content.

4.5 Harmonic Generation

This example illustrates a multifrequency simulation for a single set of parameters (i.e., *scan_p = .false.*). The spectrum is specified by setting the value of 'freq_max' to 20.e09 (i.e., 20 GHz). With 'freq0', 'delfreq', and 'freq_min' all equal to 5.e09, the spectrum will consist of the following frequencies: 5 GHz, 10 GHz, 15 GHz, and 20 GHz. Namelist 'rad' appears below.

```
$rad
   freq0 = 5.e9,
   delfreq = 5.e9,
   freq_max = 20.e9,
   freq_min = 5.e9,
   pow_in = 2.4e-03,3*0.
   phase_in = 4*0.,
   QB = 4*.0,
   phase_B = 4*0.,
   gated_I = .false.,
   sin_2 = .true.,
   AveI_pkI = .60,
$end
```

Note that we have increased the number of entries for arrays 'pow_in', 'phase_in', 'QB', and 'Phase_B' so that it corresponds to the **number of signals in the spectrum**. Had we desired to inject a signal at the second harmonic (10 GHz), we would have entered the corresponding values of input power and phase as the second elements of arrays 'pow_in' and 'phase_in', respectively. Additionally, for this run we included five space charge harmonics. Figure 7 plots 'axial'.

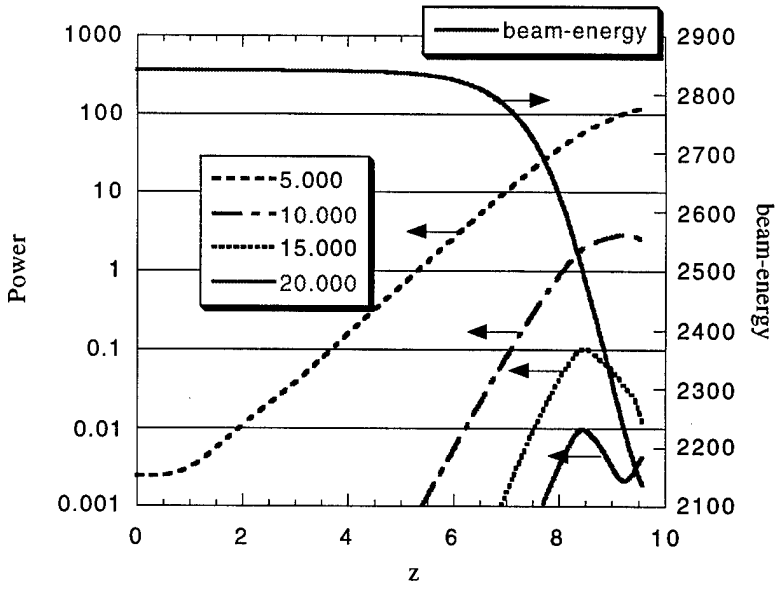

Fig. 7 — File 'axial': power in various frequencies and average beam energy vs z

4.6 Multifrequency Simulation

This example shows the results of a large scale multifrequency simulation; CHRISTINE was designed for just this type of simulation. Namelist 'rad' is modified as shown below.

```
$rad
    freq0 = 5.e9,
    delfreq = 1.e9,
    freq_max = 15.e9,
    freq_min = 1.e9,
     pow_in = 4*0.,2*2.4e-03,9*0.
    phase_in = 15*0.,
    QB =15*.0,
    phase_B = 15*0.,
    gated_I = .false.,
    sin_2 = .true.,
    AveI_pkI = .60,
 $end
```

The spectrum consists of 15 frequencies spaced 1 GHz apart starting from 1 GHz and extending to 15 GHz. Thus, 15 entries are required for each array connected with the input signal. In this case, the fifth and sixth elements of the input power corresponding to 5 GHz and 6 GHz are driven at 2.4×10^{-3} W. Not shown is namelist 'num', where parameter 'np0' has been reduced to 71. With the 15 frequency components, a total of 1562 entrance times are available. If more entrance times are

required, the value of parameter 'nnp' that appears in the parameter statement of each subroutine must be increased.

Figure 8 plots the contents of file 'P_out'. The intermodulation between the 5 GHz and 6 GHz signal is apparent in that signals are present at every integer frequency.

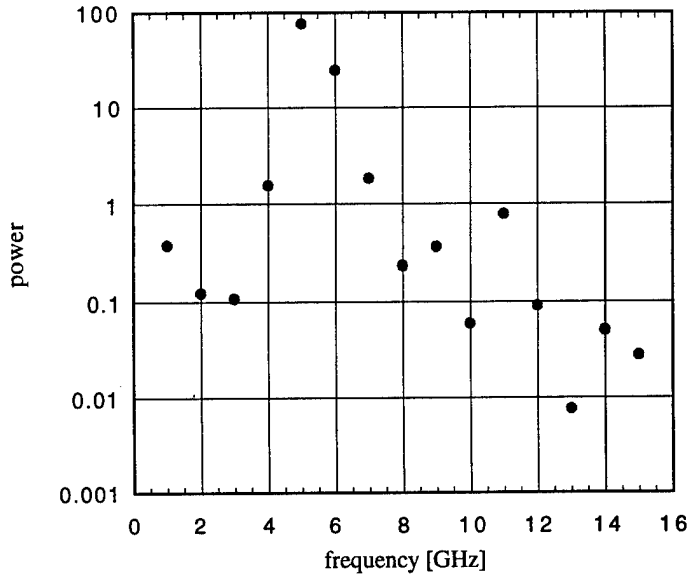

Fig. 8 — Contents of output spectrum 'P_out'

Figure 9 is an example of a phase space plot ('PS.03') for this multifrequency simulation. Here, variable θ, which spans 2π, represents the arrival time of a particle at z = 9.0 cm (ps_z(3) = 9.0) times the angular frequency separation $\Delta\omega$. The dominance of the 5 GHz signal in the output (Fig. 8) is evidenced by the apparent m = 5 periodicity in the phase space.

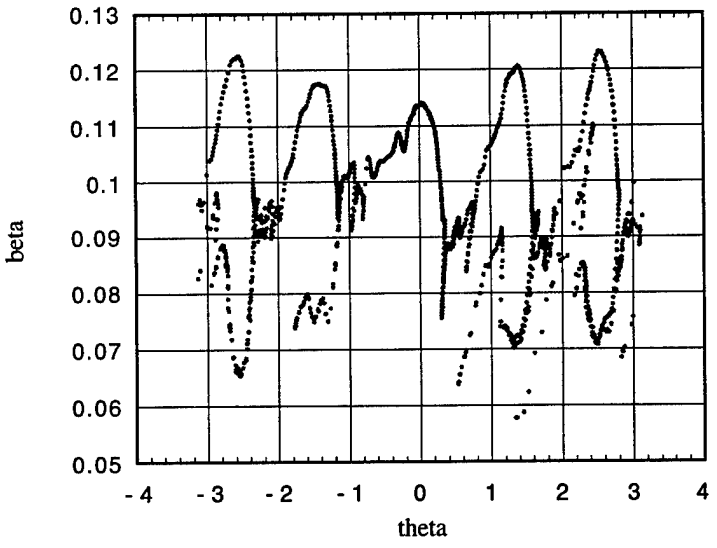

Fig. 9 — Contents of 'PS.03' showing phase space at z = 9.0 cm

Finally, Fig. 10 displays on a single set of axes the content of files 'dispersion' and 'impedance'. These show the characteristics of the structure as calculated in the sheath helix approximation (see Section 4.1).

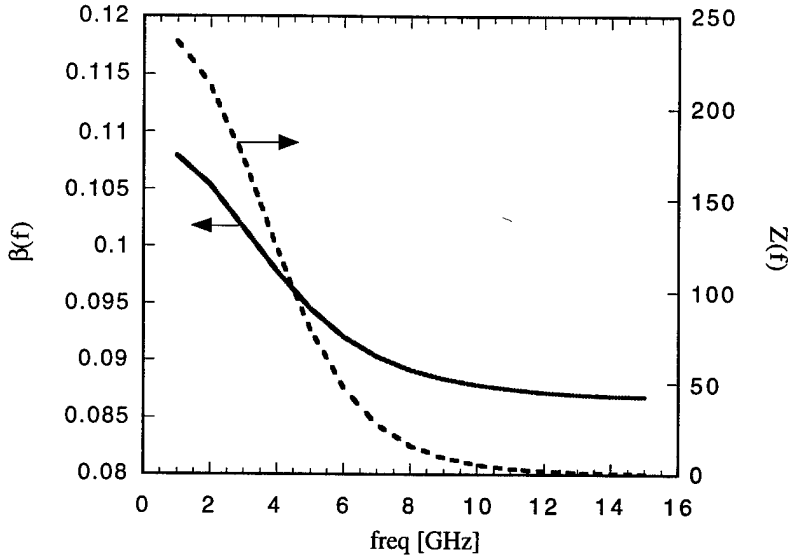

Fig. 10 — Phase velocity and impedance vs frequency

4.7 Tapering

An example of a tapered structure with attenuation is illustrated by making the following changes to namelists 'struct', 'helix_par', and 'loss_par'.

```
$struct
   zint    = 9.5758,
   zr      = 0. ,7., 8., 10.,
   dvbeam  = 4*0.
   use_sh  = .true.,
$end


$helix_par
   RH = 4*.12446,
   H_LMDA = 2*.080137,.07212,.06491
   RW = 4*.2794,
   EPS_R = 4*1.75,
   RV = 4*.2794,
   use_cor = .false.
 $end
```

```
$loss_par
   za = 0.,2.,4.,6.,8.,10.,
   att =2*1.,5.,3*1.
   dB_cm = .true.
   f_scale = 0.
 $end
```

The parameters of the structure are defined at four different points: z = 0, 7, 8, and 10 cm. The parameter that varies is the helix period 'H_LMDA'. Between z = 0 and z = 7 cm, it is equal to 0.080137 cm. It then varies linearly to a value of 0.07212 cm at z = 8 cm and then to 0.06491 at z = 10 cm. Attenuation is similarly defined. The attenuation is 1 dB/cm for $0 < z < 2$ cm. It then makes a linear tansition to a value of 5 db/cm at z = 4 cm. It then transitions back to 1 dB/cm by z = 6 cm and remains at that value throughout the remainder of the interaction region.

Files 'dispersion' and 'impedance' now contain a number of columns giving the frequency dependence of the relevant quantities at each of the four points (z = 0, 7, 8, and 10 cm). Table 2 shows the output of file 'dispersion'.

Due to the attenuation, the device output power is somewhat lower than in the previous examples. Figure 11 plots the contents of file 'P_out'.

Table 2 — Contents of File 'Dispersion': Phase Velocity vs Frequency at Four Points Along the Structure

freq [GHz]	0	1	2	3
.1000E+01	.1079E+00	.1079E+00	.9714E-01	.8735E-01
.2000E+01	.1053E+00	.1053E+00	.9428E-01	.8425E-01
.3000E+01	.1016E+00	.1016E+00	.9045E-01	.8034E-01
.4000E+01	.9779E-01	.9779E-01	.8672E-01	.7687E-01
.5000E+01	.9448E-01	.9448E-01	.8381E-01	.7441E-01
.6000E+01	.9200E-01	.9200E-01	.8179E-01	.7284E-01
.7000E+01	.9027E-01	.9027E-01	.8047E-01	.7187E-01
.8000E+01	.8909E-01	.8909E-01	.7962E-01	.7128E-01
.9000E+01	.8830E-01	.8830E-01	.7907E-01	.7090E-01
.1000E+02	.8777E-01	.8777E-01	.7871E-01	.7067E-01
.1100E+02	.8740E-01	.8740E-01	.7847E-01	.7051E-01
.1200E+02	.8714E-01	.8714E-01	.7831E-01	.7041E-01
.1300E+02	.8696E-01	.8696E-01	.7819E-01	.7034E-01
.1400E+02	.8684E-01	.8684E-01	.7812E-01	.7030E-01
.1500E+02	.8675E-01	.8675E-01	.7806E-01	.7026E-01

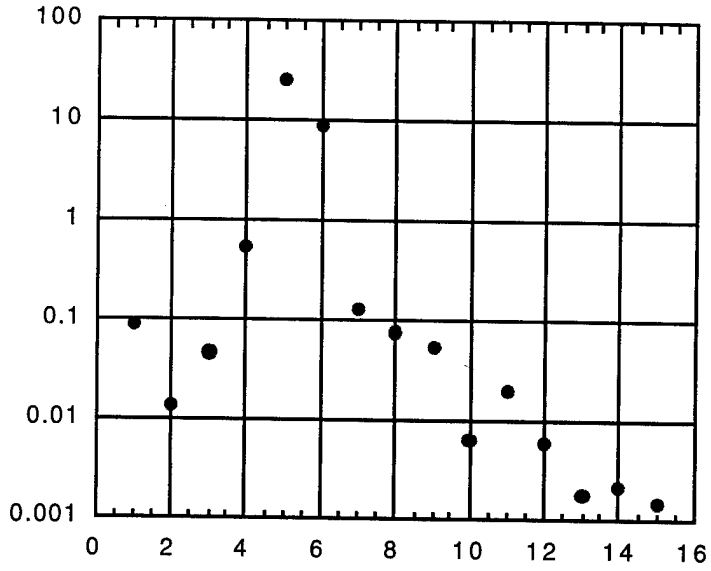

Fig. 11 — File 'P_out': the output spectrum for the case with tapering and attenuation

4.8 Importing Data

Instead of using the sheath helix model to calculate the dispersive properties of the structure, one may wish to import data for a particular structure. This is done by setting the logical variable 'use_sh' in 'struct' to 'false'. Data can now be entered through namelist 'dis_dat', or if the dispersion data is contained in files (named 'my.bp' and 'my.zc'), these may be read in as well.

We first discuss the case in which the relevant data is entered directly into namelist 'dis_dat'. A sample appears below. Data is entered in the form of a set of arrays giving frequencies, phase velocities, and impedances, each with 'npts' entries. The frequencies **need not correspond** one to one to the input signals specified in 'rad', however they must span the range of frequencies 'freq_min' to 'freq_max'. The code will interpolate phase velocity and impedance between given values if necessary. If the structure is tapered, namelist 'dis_dat' enables the user to enter the tapering profile through the use of arrays 'fract_bp' and 'fract_Z'. Below is an example of a namelist using the dispersion and impedance data displayed in Fig. 11 along with a quick and dirty (Q&D) prescription of tapering designed to model the previous example that illustrated tapering using the sheath helix model.

```
$dis_dat
   npts = 15,
   f_in =
 1.e09,2.e09,3.e09,4.e09,5.e09,6.e09,7.e09,8.e09,9.e09,10.e09,11.e09,12.e09,13.e09,14e09,15.e09,
   bp_in =
0.10790,0.10530,0.10160,0.097790,0.094480,0.092000,0.090270,0.089090,0.088300,0.087770,0.0
87400,0.087140,0.086960,0.086840,0.086750
   z_in =
```

236.40,212.30,172.00,123.20,78.920,47.030,27.090,15.430,8.8040,5.0490,2.9170,1.6970,0.99390,0
.58570,0.34710

fract_bp =2*1.,.89,.79

fract_Z = 2*1.,.84,.68

RH_eff = .12446,

use_data = .false.,

$end

The values of array 'fract_bp' are chosen so that the profile of the phase velocity at 5 GHz matches that displayed in the table in the previous example. Similarly, the elements of 'fract_Z' are picked to match the coupling impedance at 5 GHz of the previous example. Figure 12 provides a comparison of the dispersion and coupling impedance at the end of the structure using the sheath helix model with tapered parameters (the previous example) and the imported data with the Q&D tapering procedure.

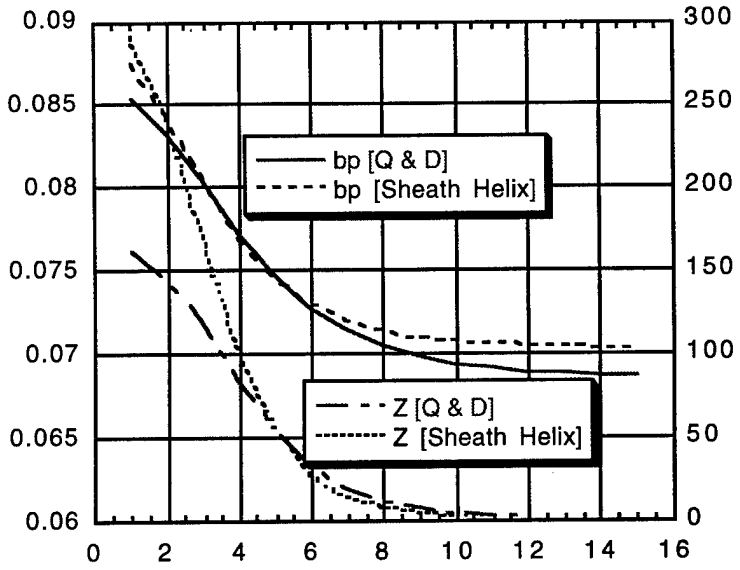

Fig. 12 — Comparison of structure data for sheath helix model and Q&D tapering

As can be seen, the Q&D method succeeds as designed in producing the correct values of impedance and phase velocity at 5 GHz. However, the parameters do not match at other frequencies. The effect this has on the output spectrum is displayed in Fig. 13.

If the Q&D method does not meet the user's needs, tapered dispersion and impedance data may be imported directly. To do this, the logical 'use_data' must be set to true and the code must be supplied with the two files 'my.bp' and 'my.zc' in the format shown in Table 3. As an example, the table can be used to import the 'correct' sheath helix data into the code; the user, of course, would supply data generated by some other means.

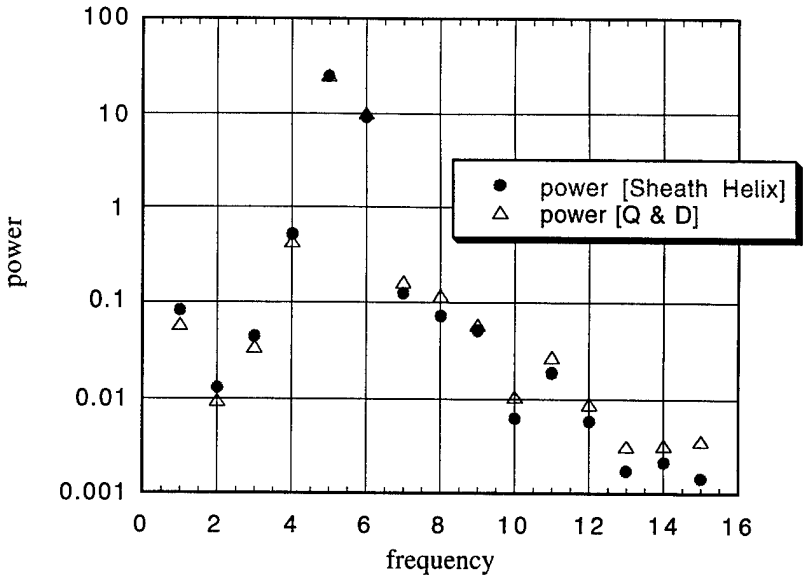

Fig. 13 — Comparison of output spectrum for two methods of introducing tapered parameters

Table 3 — Sheath Helix-generated Data in the Format to be Read as 'my.bp'

freq [GHz]	0	1	2	3
.1000E+10	.1079E+00	.1079E+00	.9714E-01	.8735E-01
.2000E+10	.1053E+00	.1053E+00	.9428E-01	.8425E-01
.3000E+10	.1016E+00	.1016E+00	.9045E-01	.8034E-01
.4000E+10	.9779E-01	.9779E-01	.8672E-01	.7687E-01
.5000E+10	.9448E-01	.9448E-01	.8381E-01	.7441E-01
.6000E+10	.9200E-01	.9200E-01	.8179E-01	.7284E-01
.7000E+10	.9027E-01	.9027E-01	.8047E-01	.7187E-01
.8000E+10	.8909E-01	.8909E-01	.7962E-01	.7128E-01
.9000E+10	.8830E-01	.8830E-01	.7907E-01	.7090E-01
.1000E+11	.8777E-01	.8777E-01	.7871E-01	.7067E-01
.1100E+11	.8740E-01	.8740E-01	.7847E-01	.7051E-01
.1200E+11	.8714E-01	.8714E-01	.7831E-01	.7041E-01
.1300E+11	.8696E-01	.8696E-01	.7819E-01	.7034E-01
.1400E+11	.8684E-01	.8684E-01	.7812E-01	.7030E-01
.1500E+11	.8675E-01	.8675E-01	.7806E-01	.7026E-01

The elements of Table 3 ('my.bp') are separated by blank spaces and each line is terminated with a carriage return. The code then produces results that are identical to those of the tapering example using the sheath helix option.

ACKNOWLEDGMENTS

This work was supported by the Office of Naval Research.

REFERENCES

1. J.E. Rowe, *Nonlinear Electron-Wave Interaction Phenomena* (Academic Press, New York, 1965).

2. H.K. Detweiler, "Characteristics of Magnetically Focused Large Signal Traveling Wave Amplifiers," Ph. D. Thesis, University of Michigan (1968).

3. N.J. Dionne, "Harmonic Generation in Octave Bandwidth Traveling-Wave Tubes," *IEEE Trans. Electron. Dev.* **ED 4**, 365 (1970).

4. A.J. Giarola, "A Theoretical Description for the Multiple-Signal Operation of a TWT," *IEEE Trans. Electron. Dev.* **ED15**, 381 (1968).